

---

# Self-Trained One-class Classification for Unsupervised Anomaly Detection

---

Jinsung Yoon, Kihyuk Sohn, Chun-Liang Li, Sercan Ö. Arık, Chen-Yu Lee, Tomas Pfister  
Google Cloud AI  
Sunnyvale, CA  
{jinsungyoon, kihyuks, chunliang, soarik, chenylee, tpfister}@google.com

## Abstract

Anomaly detection (AD), separating anomalies from normal data, has various applications across domains, from manufacturing to healthcare. While most previous works have shown to be effective for cases with fully or partially labeled data, they are less practical for AD applications due to tedious data labeling processes. In this work, we focus on *unsupervised* AD problems whose entire training data are unlabeled and may contain both normal and anomalous samples. To tackle this problem, we build a robust one-class classification framework via data refinement. To refine the data accurately, we propose an ensemble of one-class classifiers, each of which is trained on a disjoint subset of training data. Moreover, we propose a self-training of deep representation one-class classifiers (STOC) that iteratively refines the data and deep representations. In experiments, we show the efficacy of our method for unsupervised anomaly detection on benchmarks from image and tabular data domains. For example, with a 10% anomaly ratio on CIFAR-10 data, the proposed method outperforms state-of-the-art one-class classification method by 6.3 AUC and 12.5 average precision.

## 1 Introduction

Anomaly detection (AD), distinguishing anomalies from normal data, is an important problem with many applications, such as detecting faulty products using visual sensors in manufacturing, fraudulent behaviors at credit card transactions, or adversarial outcomes at intensive care units.

Given a wide range of application scenarios, AD has been studied under various settings with their own challenges based on the availability of negative (normal) and positive (anomalous) data and their labels at training. For example, when entire positive and negative data are available with their labels (Fig. 1(a)), the challenge comes from the imbalance in label distributions [13, 17, 24, 4, 27, 30]. When only negative labeled data is available (Fig. 1(b)), we often cast it as a one-class classification problem [38, 43, 36, 23, 20, 41, 28]. Their formulations have been thereby extended to accommodate unlabeled data (Fig. 1(c,d,e)) [15, 46, 8, 21, 37]. We refer to Section 2 for comprehensive review.

While there exist many prior works on these settings, they require some labeled data, which could be tedious to obtain. Despite their practical importance, unsupervised anomaly detection problem (Fig. 1(f)), whose training data is entirely unlabeled and may contain both negative and positive, has been under-explored. Some recent studies [48, 5] have evaluated their one-class classifiers for unsupervised AD settings, but their performance has been suboptimal. To illustrate this, we evaluate the unsupervised AD performance of state-of-the-art deep one-class classifier [41] with different anomaly ratios in unlabeled training data. As shown in Fig. 2, the average precision significantly drops even when a small portion (2%) of training data is contaminated with anomalies.

In this paper, we focus on *unsupervised* anomaly detection problems, where only unlabeled data that may include both negative and positive samples are available during training. Given the impressive

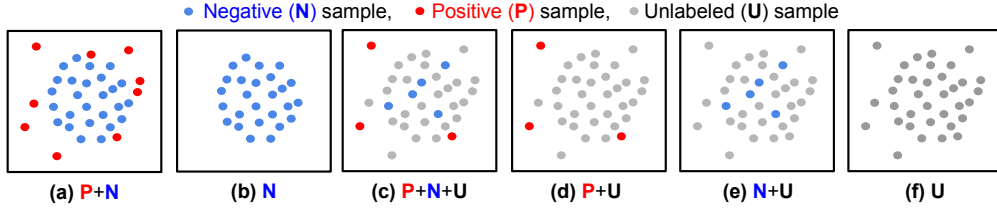


Figure 1: Anomaly detection problem settings. Blue and red are for **labeled** negative (normal) and positive (anomalous) samples, respectively. Grey dots denote **unlabeled** samples. While previous works mostly focus on supervised (a, b) or semi-supervised (c, d, e) settings, we tackle an anomaly detection using only unlabeled data (f) that may contain both negative and positive samples.

performance of one-class classifiers trained on negative samples [20, 23, 5, 41, 28], our goal is to utilize them, and improve their performance by refining the unlabeled training data so as to adopt learning strategies of one-class classification for unsupervised anomaly detection. Inspired by the recent success of self-training in learning without labels [7, 45], we propose a novel self-trained one-class classification (STOC) framework. We illustrate STOC built on a two-stage framework of deep one-class classifiers [41, 28] in Fig. 3. STOC iteratively trains deep representations using refined data while improving refinement of unlabeled data by excluding potential positive (anomalous) samples. For the data refinement process, we employ an ensemble of one-class classifiers, each of which is trained on a different subset of unlabeled training data, and dictate samples as normal with the consensus of all the classifiers. The refined training data are used to train the final one-class classifier to generate the anomaly scores in the unsupervised setting. Note that the representation learning part is optional in the STOC framework; in other words, any shallow [38] or deep representation one-class classifiers [41, 28] can benefit from the proposed framework (see Fig. 7 in Section 4.3.2). Unlike previous works [48, 36, 20, 23, 5, 41, 28], STOC works under realistic assumptions that majority of the training data is negative – human labeling can be completely removed from the entire process.

We conduct extensive experiments across various datasets from different domains, including semantic AD (CIFAR-10 [25], Dog-vs-Cat [16]), manufacturing AD (MVTec AD [6]), and tabular AD. We study methods from shallow ([38, 31]) to deep ([41, 28, 5]) models. By evaluating at different anomaly ratios of unlabeled training data, we show that STOC significantly boosts the performance of one-class classifiers. For example, in Fig. 2, STOC improves more than 15 average precision (AP) with the 10% anomaly ratio upon one-class contrastive representation [41] on CIFAR-10. Similarly, on MVTec AD, STOC retains a strong performance, dropping less than 1 AUC with 10% anomaly ratio, while the best existing one-class classifiers [28] drops more than 6 AUC. We further investigate the efficacy of our design choices, such as numbers of ensemble classifiers, thresholds, or refinement of deep representations via ablation study.

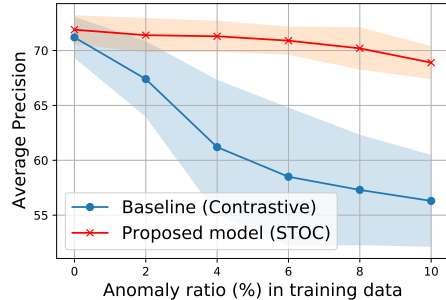


Figure 2: Performance of our proposed model and baseline one-class classifier using contrastive representation [41] on CIFAR-10 with various anomaly ratios in the training data.

## 2 Related Work

We review existing works under different settings as described in Fig. 1 and discussed their challenges.

**Positive + Negative setting** is often considered as a supervised binary classification problem. The challenge arises due to the imbalance in label distributions as positive (anomalous) samples are rare. As summarized in [10], to address this, over-/under-sampling [13, 17], weighted optimization [24, 4], synthesizing data of minority classes [27, 30], and hybrid methods [18, 2] have been studied.

**Negative setting** is often converted to a one-class classification problem, with the goal of finding a decision boundary that includes as many one-class samples as possible. Shallow models for this setting include one-class support vector machines [38] (OC-SVM), support vector data description [43] (SVDD), kernel density estimation (KDE) [26], and Gaussian density estimation (GDE) [35]. There

are also auto-encoder based models [47] that treat the reconstruction error as the anomaly score. In recent years, deep learning based one-class classifiers have been developed, such as deep one-class classifier [36], geometric transformation [20], or outlier exposure [23]. Noting the degeneracy or inconsistency of learning objectives of existing end-to-end trainable deep one-class classifiers, [41] has proposed a deep representation one-class classifier, a two-stage framework that learns self-supervised representations [19, 14] followed by shallow one-class classifiers, and has been extended for texture anomaly localization with CutPaste [28]. The robustness of these methods under unsupervised setting has also been shown in part [48, 5] when the anomaly ratio is very low.

**Semi-supervised setting** is defined as utilizing small labeled samples and large unlabeled samples to distinguish anomalies from normal data. Depending on which labeled samples are given, we categorize this setting into three sub-categories. If only some positive/negative labeled samples are provided, we denote that as a PU/NU setting. Most previous works in semi-supervised AD settings focused on NU setting where only some of the normal labeled samples are given [34, 42, 1]. PNU setting is a more general semi-supervised setting where subsets of both positive and negative labeled samples are given. Deep SAD [37] and SU-IDS [33] are included in this category. Note that in comparison to Deep SAD, which utilized some labeled data, the proposed framework significantly outperforms under multiple benchmark datasets without using any labeled data (see Section 4.2).

**Unlabeled setting** has received relatively less attention despite its significance in automating machine learning. Two of the most popular methods for this setting are isolation forest [31] and local outlier factor [11], but they are hard to scale and less compatible with recent advances in representation learning. While one-class classifiers, such as OC-SVM, SVDD, or their deep counterparts, apply to unlabeled settings by assuming the data is all negative, and the robustness of those methods has also been demonstrated in part [48, 5], in practice we observe a significant performance drop with a high anomaly ratio, as shown in Fig. 2. Our proposed framework mostly recovers the lost performance of state-of-the-art shallow and deep one-class classifiers trained on unlabeled data.

**Self-training** [39, 32] is an iterative training mechanism using machine-generated pseudo labels as targets to train machine learning models. It has regained popularity recently with its successful applications to semi-supervised image classification [7, 40, 45]. Improving the quality of pseudo labels using an ensemble of classifiers is also studied. [12] trains an ensemble of classifiers with different classification algorithms to make a consensus for noisy label verification. Co-training [9] trains multiple classifiers, each of which is trained on the distinct views, to supervised other classifiers. Co-teaching [22] and DivideMix [29] share a similar idea in that they both train multiple deep networks on separate data batches to learn different decision boundaries, thus become useful for noisy label verification. While sharing a similarity, to our knowledge, we are the first to apply self-training to *unsupervised* learning of an anomaly detector, with no human-generated labels.

### 3 Self-Trained One-class Classifier (STOC)

In this section, we describe our proposed framework for unsupervised anomaly detection. Similarly to the self-training framework for semi-supervised learning [7], our **Self-Trained One-class Classifier (STOC)** is an iterative training method, where we refine the data (Section 3.1) and update the representation with refined data (Section 3.2), followed by building a one-class classifier using refined data and representations, as described in Algorithm 1 and Fig. 3. Note that the framework is amenable to use fixed (e.g., raw or pretrained) representations – in this case, the framework would be composed of a single step of data refinement followed by building an one-class classifier using refined data.

**Notation.** We denote the training data as  $\mathcal{D} = \{\mathbf{x}_i\}_{i=1}^N$  where  $\mathbf{x}_i \in \mathcal{X}$  and  $N$  is the number of training samples.  $y_i \in \{0, 1\}$  is the corresponding label to  $\mathbf{x}_i$ , where 0 denotes normal (negative) and 1 denotes anomaly (positive). Note that labels are not provided in the unsupervised setting.

Let us denote a feature extractor as  $g : \mathcal{X} \rightarrow \mathcal{Z}$ .  $g$  may include any data preprocessing functions, an identity function (if raw data is directly used for one-class classification), and learned or learnable representation extractors such as deep neural networks. Let us define a one-class classifier as  $f : \mathcal{Z} \rightarrow [-\infty, \infty]$  that outputs anomaly scores of the input feature ( $g(\mathbf{x})$ ). Higher the score  $f(g(\mathbf{x}))$ , more anomalous the sample  $\mathbf{x}$  is, and the binary prediction is made by thresholding:  $\mathbb{1}(f(g(\mathbf{x})) \geq \eta)$ .

#### 3.1 Data Refinement

A naive way to generate pseudo labels of unlabeled data is to construct a one-class classifier on raw or learned representations (e.g., [41]) and threshold the anomaly score to obtain a binary label of

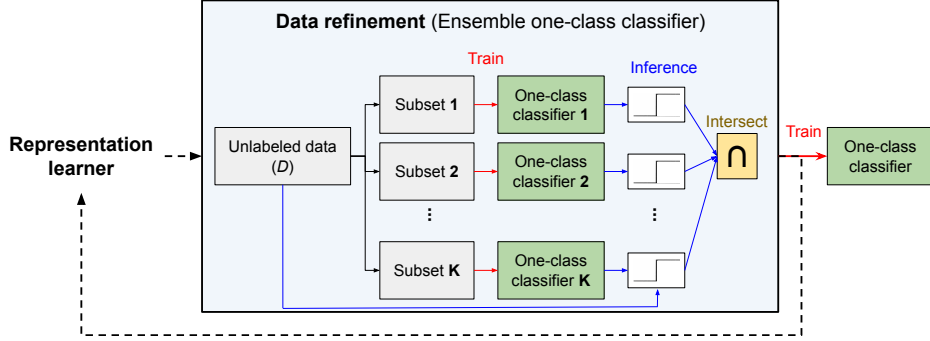


Figure 3: Block diagram of STOC composed of representation learner (Section 3.2), data refinement (Section 3.1), and the final one-class classifier blocks. Representation learner updates the deep models using refined data from the data refinement block, but is optional if using fixed representations. Data refinement is done by ensemble one-class classifiers, each of which is trained on  $K$  disjoint subsets of unlabeled training data. Samples predicted as normal by all classifiers are retained in the refined data.

normal and anomalous. As we update the model with refined data that excludes samples predicted as positive, it is important to generate pseudo labels of training data as accurately as possible.

To this end, instead of training a single classifier, we train an ensemble of  $K$  one-class classifiers and aggregate their predictions to generate pseudo labels. We illustrate the data refinement block in Fig. 3 and as REFINEDATA in Algorithm 1. Specifically, we randomly divide the unlabeled training data  $\mathcal{D}$  into  $K$  disjoint subsets  $\mathcal{D}_1, \dots, \mathcal{D}_K$ , and train  $K$  different one-class classifiers ( $f_1, \dots, f_K$ ) on corresponding subsets ( $\mathcal{D}_1, \dots, \mathcal{D}_K$ ). Then, we predict a binary label of the data  $\mathbf{x}_i \in \mathcal{D}$  as follows:

$$\hat{y}_i = 1 - \prod_{k=1}^K \left[ 1 - \mathbb{1}(f_k(g(\mathbf{x}_i)) \geq \eta_k) \right] \quad (1)$$

$$\eta_k = \max \eta \text{ s.t. } \frac{1}{N} \sum_{i=1}^N \mathbb{1}(f_k(g(\mathbf{x}_i)) \geq \eta) \geq \gamma \quad (2)$$

where  $\mathbb{1}(\cdot)$  is the indicator function that outputs 1/0 if the input is True/False.  $f_k(g(\mathbf{x}_i))$  represents an anomaly score of  $\mathbf{x}_i$  for a one-class classifier  $f_k$ .  $\eta_k$  in Eq. (2) is a threshold determined as a  $\gamma$  percentile of the anomaly score distribution  $\{f_k(g(\mathbf{x}_i))\}_{i=1}^N$ .

To interpret Eq. (1),  $\mathbf{x}_i$  is predicted as normal, i.e.,  $\hat{y}_i = 0$ , if all  $K$  one-class classifiers predict it as normal. While this may be too strict and potentially reject many true normal samples in the training set, we find that in practice it is more critical to be able to exclude true anomalous samples from the training set. The effectiveness of the ensemble classifier is empirically shown in Section 4.3.

### 3.2 Representation Update

STOC follows the idea of deep representation one-class classifiers [41], where in the first stage deep neural network is trained with self-supervision, such as rotation prediction [20], contrastive [41], or CutPaste [28], to provide meaningful representations of the data, and in the second stage off-the-shelf one-class classifiers are trained on these learned representations. Such a two-stage framework is shown to be beneficial as it prevents the degeneracy of the deep one-class classifiers [36].

Here, we propose to conduct self-supervised representation learning jointly with the data refinement. More precisely, we train a trainable feature extractor  $g$  using  $\hat{\mathcal{D}} = \{\mathbf{x}_i : \hat{y}_i = 0\}$ , a subset of unlabeled data  $\mathcal{D}$  that includes samples whose predicted labels with an ensemble one-class classifier from Section 3.1 are negative. We also update  $\hat{\mathcal{D}}$  as we proceed the representation learning. The proposed method is illustrated in Algorithm 1 as STOC. In contrast to previous work [41, 28] that use the entire training data for learning self-supervised representation, we find it necessary to refine the training data even for learning deep representations. Without representation refinement, the performance improvements of STOC are limited, as shown in Section 4.3.2.

Following representation learning, we train a one-class classifier on refined data  $\hat{\mathcal{D}}$  using updated representation by  $g$  for test time prediction, as in line 13, 14 in Algorithm 1.

---

**Algorithm 1** STOC: Self-Trained One-class Classifier.

---

**Input:** Training data  $\mathcal{D} = \{\mathbf{x}_i\}_{i=1}^N$ , Ensemble count ( $K$ ), threshold ( $\gamma$ )

**Output:** Refined data ( $\hat{\mathcal{D}}$ ), trained one-class classifier ( $f$ ), feature extractor ( $g$ )

```
1: function REFINEDATA( $\mathcal{D}, g, K, \gamma$ )
2:   Train OCC models  $\{f_k\}_{k=1}^K$  on  $\{\mathcal{D}_k\}_{k=1}^K$ ,  $K$  disjoint subsets of the training data  $\mathcal{D}$ .
3:   Compute thresholds  $\eta_k$ 's for  $\gamma$  percentile of anomaly distributions (Eq. (2)).
4:   Predict binary labels  $\hat{y}_i$  (Eq. (1)).
5:   Return  $\hat{\mathcal{D}} = \{\mathbf{x}_i : \hat{y}_i = 0, \mathbf{x}_i \in \mathcal{D}\}$ .
6: end function
7: function STOC( $\mathcal{D}, K, \gamma$ )
8:   Initialize the feature extractor  $g$ .
9:   while  $g$  not converged do
10:     $\hat{\mathcal{D}} = \text{REFINEDATA}(\mathcal{D}, g, K, \gamma)$ .
11:    Update  $g$  using  $\hat{\mathcal{D}}$  with self-supervised learning objectives.
12:   end while
13:    $\hat{\mathcal{D}} = \text{REFINEDATA}(\mathcal{D}, g, K, \gamma)$ .
14:   Train an OCC model ( $f$ ) on refined data ( $\hat{\mathcal{D}}$ ).
15: end function
```

---

### 3.3 Selecting hyperparameters

As STOC is designed for unsupervised anomaly detection, labeled validation data for hyperparameter tuning is typically not available. In this section, we provide insights on how to select important hyperparameters. Later in Section 4.3.1, we also provide sensitivity analyses on these hyperparameters.

Our data refinement block introduces two hyperparameters: the number of one-class classifiers ( $K$ ) and the percentile threshold ( $\gamma$ ). First, there is a trade-off between the number of classifiers for ensemble and the size of disjoint subsets for training each classifier. For example, with large  $K$ , we aggregate prediction from many classifiers, each of which may contain more randomness. However, it comes at a cost of reduced performance per classifier as we use smaller subsets to train them. In practice, we find  $K = 5$  works well across different datasets and anomaly ratios in unlabeled training data. Second,  $\gamma$  controls the purity and coverage of refined data. If  $\gamma$  is large and thus classifiers reject too many samples, the refined data could be more pure and contain mostly the normal samples; however, the coverage of the normal samples would be limited. On the other hand, with small  $\gamma$ , the refined data may still contain many anomalies and the performance improvement with STOC would be limited. As such, the performance of STOC could be suboptimal if the true anomaly ratio is not available. Nevertheless, in our experiments, we observe that STOC is robust to selection of  $\gamma$  when chosen between the true anomaly ratio and the twice of that. This suggests that it is safer to use  $\gamma$  with an over-estimate of true anomaly ratio.

## 4 Experiments

In this section, we test the efficacy of our proposed self-training framework for unsupervised anomaly detection tasks on tabular (Section 4.1) and image (Section 4.2) domains. We evaluate the methods with varying ratios of anomaly samples in unlabeled training data and with different combinations of representation learning and one-class classifiers. In Section 4.3, we provide an ablation study to better understand sources of gain, as well as sensitivity analyses to multiple hyperparameters.

**Implementation details:** to reduce the computational complexity of data refinement block, we utilize simple one-class classifier such as GDE as the OCC in the data refinement block. In two-stage model, we only update data refinement block at 1st, 2nd, 5th, 10th, 20th, 50th, 100th, 500th epochs instead of every epoch. After 500 epochs, we update the data refinement block per each 500th epoch. Each run of experiments requires a single V100 GPU.

### 4.1 Experiments on Tabular Domain

**Datasets.** Following [48, 5], we test the efficacy of STOC on a variety of tabular datasets, including KDDCup, Thyroid, or Arrhythmia from UCI repository [3]. We also use KDDCup-Rev, where the

labels of KDDCup is reversed so that attack represents anomaly [48]. To construct data splits, we use 50% of normal samples for training. In addition, we take anomaly samples worthy of the 10% of the normal samples in the training set. This allows to simulate unsupervised settings with anomaly ratio of up to 10% of entire training set. The rest of the data is used for testing.<sup>1</sup> We conduct experiments using 5 random splits and 5 random seeds. We report the average and standard deviation of 25 F1-scores (with scale 0-100) for the performance metric.

**Models.** We re-implement GOAD [5], a type of augmentation prediction methods [19, 41] with random projections for learning representations, for the baseline with a few modifications. First, instead of using embeddings to compute the loss, we use a parametric classifier, similarly to the augmentation prediction [41]. Second, we follow the two-stage framework [41] to construct deep one-class classifiers. For N setting, our implementation achieves 98.0 for KDD, 95.0 for KDD-Rev, 75.1 for Thyroid, and 54.8 for Arrhythmia F1-scores, which are comparable to those reported in [5]. Please see Appendix A.3 for formulation and implementation details.

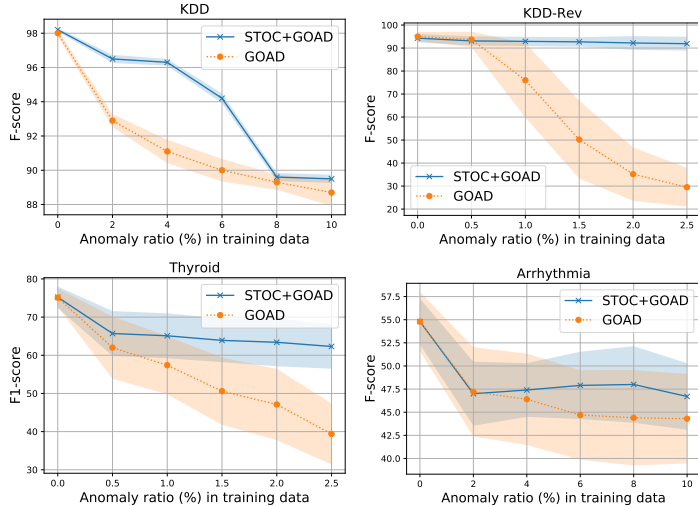


Figure 4: Unsupervised anomaly detection performance (F1-score) using GOAD [5] and that with STOC on various tabular datasets. Shaded areas represent the standard deviation.

**Results.** We show results of GOAD and GOAD with STOC in Fig. 4. The ranges of the noise ratio are set as 0% to the anomaly ratios in the original dataset (if anomaly ratios are larger than 10%, we set the maximum anomaly ratio as 10%). For KDD-Rev, we set the maximum anomaly ratio as 2.5% because the performances of GOAD (without STOC) drop significantly even with a small amount of anomalies in the training data.

As can be seen in Fig. 4, integrating STOC significantly outperforms GOAD, the state-of-the-art method for tabular one-class classifier. The improvements are more significant especially at higher anomaly ratios. These also show the applicability of STOC to both small (Thyroid & Arrhythmia) and large datasets (KDD & KDD-Rev).

## 4.2 Experiments on Image Domain

**Datasets.** We evaluate STOC on visual anomaly detection benchmarks, including CIFAR-10 [25], f-MNIST [44], Dog-vs-Cat [16], and MVTEC anomaly detection (AD) [6]. For CIFAR-10, f-MNIST, and Dog-vs-Cat datasets, samples from one class are set to be normal and the remainders from other classes are set to be anomaly. Similarly to experiments on tabular data in Section 4.1, we swap a certain amount of the normal training data with anomalies so that the anomaly ratio reaches the target percentage for unsupervised settings. For MVTEC AD experiments, since there is no anomalous data available for training, we borrow 10% of the anomalies from the test set and swap them with normal

<sup>1</sup>Note that the experimental settings with contaminated training data in GOAD [5] and DAGMM [48] are slightly different from ours. Our contamination ratio is defined as anomaly ratio over the entire training data, while their contamination ratio is the anomaly ratio over the entire anomalies in the dataset.

samples in the training set. Note that the 10% of samples borrowed from the test set are excluded from evaluation. For all datasets, we experiment with varying anomaly ratios from 0% to 10%.

We use area under ROC curve (AUC) and average precision (AP) metrics to quantify the performance of visual anomaly detection (with scale 0-100). When computing AP, we set the minority class of the test set as label 1 and majority as label 0 (e.g., normal samples are set as label 1 for CIFAR-10 experiments as there are more anomaly samples that are from 9 classes in the test set). We run all experiments with 5 random seeds, and report the average performance for each dataset across all classes in Fig. 5 and Fig. 6. Per-class AUC and AP are reported in Appendix A.4.

**Models.** For semantic anomaly detection benchmarks, CIFAR-10, f-MNIST, and Dog-vs-Cat, we compare the STOC with two-stage one-class classifiers [41] using various representation learning methods, such as distribution-augmented contrastive learning [41], rotation prediction [19, 20] and its improved version [41], or denoising autoencoder. For MVTEC AD benchmarks, we use CutPaste [28] as a baseline and compare to its version with STOC integration. For both experiments, we use ResNet-18 model, trained from random initialization, using the hyperparameters from [41] and [28]. The same model and hyperparameter configurations are used for STOC with  $K = 5$ , the count of classifier ensembles. We set  $\gamma$  as twice the anomaly ratios of the training data. For 0% anomaly ratios, we set  $\gamma$  as 0.5. Finally, Gaussian Density Estimator (GDE) on learned representations is used for one-class classifiers.

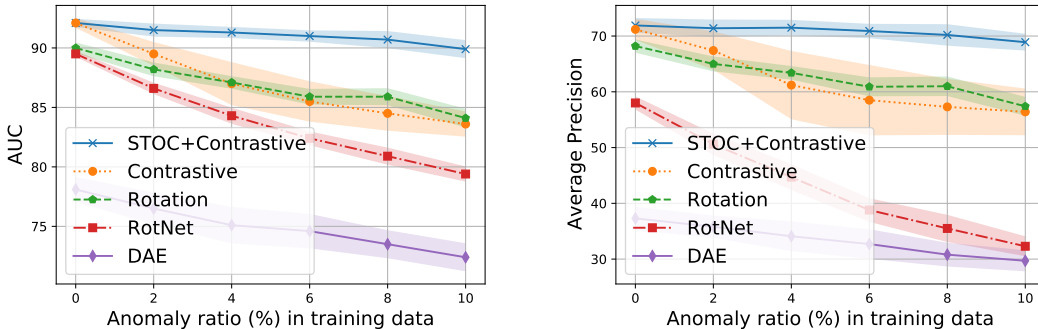


Figure 5: Unsupervised anomaly detection performance with various one-class classifiers on CIFAR-10 dataset. For STOC we adopt distribution-augmented contrastive representation learning [41]. (Left) AUC, (Right) Average Precision (AP).

**Results.** Fig. 5 shows a significant performance drop with increased anomaly ratios, regardless of the representation learning algorithms. For example, AUC of distribution-augmented contrastive representation [41] drops from 92.1 to 83.6 when anomaly ratio becomes 10%. Similarly, improved rotation prediction representation [19], though not as significant, drops from 90.0 to 84.1. On the other hand, STOC effectively handles the contamination in the training data and achieves 89.9 AUC with 10% anomaly ratio, reducing the performance drop by 74.1%. Note that the oracle performance of STOC would be perfectly removing the anomalies from the training data (which is the same as the performances at 0% anomaly ratio for the same size of the data). As can be seen in Fig. 5, the performances of STOC are similar (less than 2.5 AUC difference) with the oracle performances of STOC even with high anomaly ratios (10%). Similar trends have been observed from other metrics, such as AP in Fig. 5 or Recall at Precision of 70 and 90 in Fig. 9 in the Appendix.

We repeat experiments on 3 more visual anomaly detection datasets and report results in Fig. 6. We observe consistent and significant improvements over the baseline across different datasets and different one-class classification methods. Note that the improvement is more significant at higher anomaly ratios. For instance, on MVTEC AD dataset, STOC improves AUC by 4.9 and AP by 7.1 upon state-of-the-art CutPaste one-class classifier with anomaly ratio of 10%. In the Appendix (Section A.4), we also illustrate per-class performances of STOC compared with the state-of-the-art.

### 4.3 Ablation studies

In this section, we conduct sensitivity analyses on two hyperparameters of STOC, namely, the number  $K$  for ensemble one-class classifiers and the percentile threshold  $\gamma$  that determines normal and anomalies in the data refinement module. In addition, we show the importance of updating

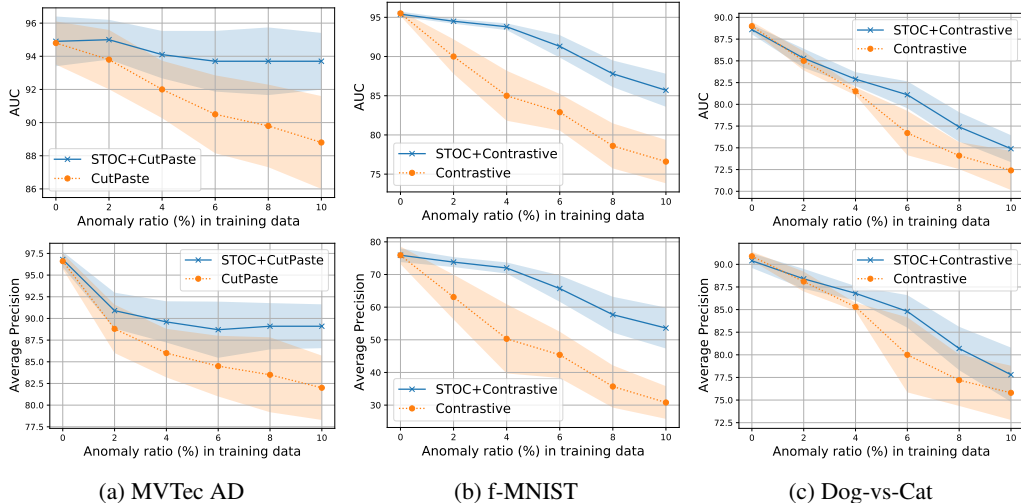


Figure 6: Unsupervised anomaly detection performance on (a) MVTec AD (b) f-MNIST, and (c) Dog-vs-Cat datasets with varying anomaly ratios. We use state-of-the-art one-class classification models for baselines, such as distribution-augmented contrastive representations [41] for f-MNIST and Dog-vs-Cat, or CutPaste [28] for MVTec AD, and build STOC on top of them.

representation with refined data. Ablation studies are conducted on two visual anomaly detection benchmarks, CIFAR-10 and MVTec AD. More results can be found in the Appendix.

#### 4.3.1 Sensitivity Analyses for Hyperparameters

Since our method is designed for solving unsupervised anomaly detection problem, it is important to ensure robust performance against changes in the hyperparameters. In Fig. 7, we present the sensitivity analyses of our method with respect to various hyperparameters.

In Fig. 7a, we observe the performance improvement as we increase the number of classifiers for ensemble. This is particularly effective on CIFAR dataset (top in Fig. 7a) where the number of samples in the training data is large enough that even with large  $K$ , the number of samples to train each OCC ( $N/K$ ) would be sufficient.

In Fig. 7b, we observe that STOC performs robustly when  $\gamma$  is set to be larger than the actual anomaly ratio (10%). When  $\gamma$  is less than 10%, however, we see a significant drop in performance, all the way to the baseline ( $\gamma = 0$ ). Our results show that STOC improves upon baseline regardless of the threshold. In addition, it suggests that  $\gamma$  could be set to be within the true anomaly ratio and the twice of it to maximize its effectiveness.

#### 4.3.2 Importance of Representation Update with Refined Data

While iterative updates of representations with refined data is important for STOC, one can easily decompose representation learning and data refinement of STOC. This would result in a three-stage framework, where we learn representations until convergence without data refinement, followed by the data refinement and learning one-class classifier. As in Fig. 7c, a STOC using a pretrained then fixed representation (i.e., data refinement is used for OCC only) already improves the performance upon the baseline with no data refinement at any stage of learning representation or classifier, in AUC by 4.9, AP by 8.0 on CIFAR-10, and AUC by 1.3, AP by 1.3 on MVTec AD. This confirms the effectiveness of our data refinement module. More results on applying STOC on raw tabular features or learned (and fixed) visual representations are provided in Appendix A.2. Moreover, we find that learning representation with refined data plays a crucial role, resulting in another improvement in AUC by 1.4, AP by 4.5 on CIFAR-10, and AUC by 3.2, AP by 4.8 on MVTec AD, upon a STOC using a fixed representation.

#### 4.4 Quantifying the Refinement Efficacy

In this section, we evaluate how many normal and anomalies are excluded via the proposed data refinement block. As in Fig. 8(a, b), with data refinement, we can exclude more than 80% of



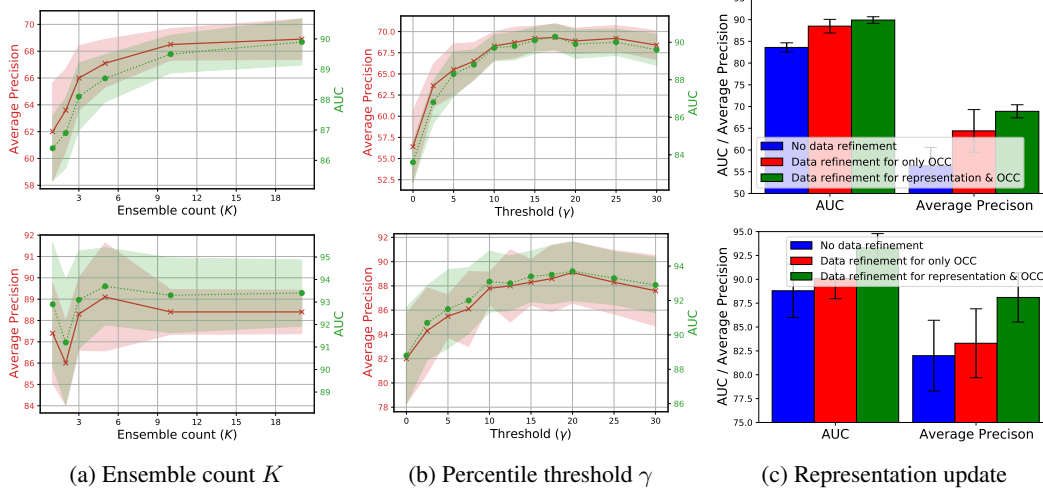


Figure 7: Ablation studies on (top) CIFAR-10 and (bottom) MVTec AD datasets under 10% anomaly ratio setting with respect to (a) ensemble count  $K$ , (b) percentile threshold  $\gamma$ , and (c) data refinement with or without representation update.

anomalies in the training set without removing too many normal samples. For instance, among 4% anomalies in CIFAR-10 data, STOC is able to exclude 80% anomalies while removing less than 20% normal samples. Such a high recall of anomalies of STOC not only is useful for unsupervised anomaly detection, but also could be useful to improve the annotation efficiency when a budget for active learning is available. Fig. 8(c, d) demonstrates the removed normal and abnormal samples by the data refinement module over training epochs. It shows that better representation learning (as training epochs increase) consistently improves the efficacy of the data refinement.

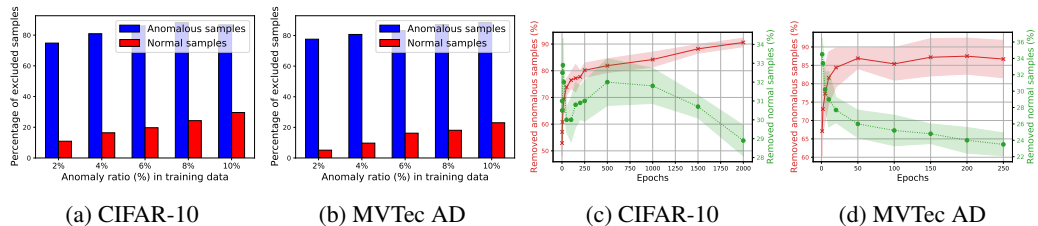


Figure 8: Percentage of excluded anomalous and normal samples by data refinement (a, b) with different anomaly ratios in training data and (c, d) over training epochs for 10% anomaly ratio.

## 5 Conclusion

Anomaly detection has wide range of practical use cases. A challenging and costly aspect of building an anomaly detection system is labeling as anomalies are rare and are not easy to detect by humans. To enable high performance anomaly detection without any labels, we propose a novel anomaly detection framework, STOC. STOC can be flexibly integrated with any one-class classifier, applied on raw data or on trainable representations. STOC employs an ensemble of multiple one-class classifiers to propose candidate anomaly samples that are refined from training, which allows more robust fitting of the anomaly decision boundaries as well as better learning of data representations. We demonstrate the state-of-the-art anomaly detection performance of STOC on multiple tabular and image data.

STOC has the potential to make huge positive impact in real-world AD applications where detecting anomalies is crucial, such as for financial crime elimination, cybersecurity advances, or improving manufacturing quality. We note the potential risk associated with using STOC that when representations are not sufficiently good, there will be a negative cycle of refinement and representation updates/one-class classifier. While we rely on the existence of good representations this may not be true for other domains (e.g., cybersecurity). This paper focuses on unsupervised setting, and demonstrates strong anomaly detection performance. This opens new horizons for human-in-the-loop anomaly detection systems that are low cost and robust. We leave these explorations to future work.

## 6 Acknowledgements

Discussions with Jeremy Kubica, Madeleine Udell, Mike Dusenberry, Clayton Mellina and Ting Yu are gratefully acknowledged.

## References

- [1] S. Akcay, A. Atapour-Abarghouei, and T. P. Breckon. Ganomaly: Semi-supervised anomaly detection via adversarial training. In *Asian conference on computer vision*, pages 622–637. Springer, 2018. 3
- [2] R. Alejo, R. M. Valdovinos, V. García, and J. H. Pacheco-Sanchez. A hybrid method to face class overlap and class imbalance on neural networks and multi-class scenarios. *Pattern Recognition Letters*, 34(4):380–388, 2013. 2
- [3] A. Asuncion and D. Newman. Uci machine learning repository, 2007. 5
- [4] S. Barua, M. M. Islam, X. Yao, and K. Murase. Mwmote—majority weighted minority oversampling technique for imbalanced data set learning. *IEEE Transactions on knowledge and data engineering*, 26(2):405–425, 2012. 1, 2
- [5] L. Bergman and Y. Hoshen. Classification-based anomaly detection for general data. *arXiv preprint arXiv:2005.02359*, 2020. 1, 2, 3, 5, 6, 14
- [6] P. Bergmann, M. Fauser, D. Sattlegger, and C. Steger. Mvtec ad—a comprehensive real-world dataset for unsupervised anomaly detection. In *Proceedings of the IEEE/CVF Conference on Computer Vision and Pattern Recognition*, pages 9592–9600, 2019. 2, 6
- [7] D. Berthelot, N. Carlini, I. Goodfellow, N. Papernot, A. Oliver, and C. Raffel. Mixmatch: A holistic approach to semi-supervised learning. *arXiv preprint arXiv:1905.02249*, 2019. 2, 3
- [8] G. Blanchard, G. Lee, and C. Scott. Semi-supervised novelty detection. *The Journal of Machine Learning Research*, 11:2973–3009, 2010. 1
- [9] A. Blum and T. Mitchell. Combining labeled and unlabeled data with co-training. In *Proceedings of the eleventh annual conference on Computational learning theory*, pages 92–100, 1998. 3
- [10] P. Branco, L. Torgo, and R. Ribeiro. A survey of predictive modelling under imbalanced distributions. *arXiv preprint arXiv:1505.01658*, 2015. 2
- [11] M. M. Breunig, H.-P. Kriegel, R. T. Ng, and J. Sander. Lof: identifying density-based local outliers. In *Proceedings of the 2000 ACM SIGMOD international conference on Management of data*, pages 93–104, 2000. 3
- [12] C. E. Brodley, M. A. Friedl, et al. Identifying and eliminating mislabeled training instances. In *Proceedings of the National Conference on Artificial Intelligence*, pages 799–805. Citeseer, 1996. 3
- [13] N. V. Chawla, K. W. Bowyer, L. O. Hall, and W. P. Kegelmeyer. Smote: synthetic minority over-sampling technique. *Journal of artificial intelligence research*, 16:321–357, 2002. 1, 2
- [14] T. Chen, S. Kornblith, M. Norouzi, and G. Hinton. A simple framework for contrastive learning of visual representations. In *International conference on machine learning*, pages 1597–1607. PMLR, 2020. 3
- [15] F. Denis. Pac learning from positive statistical queries. In *International Conference on Algorithmic Learning Theory*, pages 112–126. Springer, 1998. 1
- [16] J. Elson, J. R. Douceur, J. Howell, and J. Saul. Asirra: a captcha that exploits interest-aligned manual image categorization. In *ACM Conference on Computer and Communications Security*, volume 7, pages 366–374, 2007. 2, 6
- [17] A. Estabrooks, T. Jo, and N. Japkowicz. A multiple resampling method for learning from imbalanced data sets. *Computational intelligence*, 20(1):18–36, 2004. 1, 2

- [18] M. Galar, A. Fernandez, E. Barrenechea, H. Bustince, and F. Herrera. A review on ensembles for the class imbalance problem: bagging-, boosting-, and hybrid-based approaches. *IEEE Transactions on Systems, Man, and Cybernetics, Part C (Applications and Reviews)*, 42(4):463–484, 2011. [2](#)
- [19] S. Gidaris, P. Singh, and N. Komodakis. Unsupervised representation learning by predicting image rotations. *arXiv preprint arXiv:1803.07728*, 2018. [3](#), [6](#), [7](#), [13](#), [14](#)
- [20] I. Golan and R. El-Yaniv. Deep anomaly detection using geometric transformations. *arXiv preprint arXiv:1805.10917*, 2018. [1](#), [2](#), [3](#), [4](#), [7](#), [13](#), [14](#)
- [21] N. Görnitz, M. Kloft, K. Rieck, and U. Brefeld. Toward supervised anomaly detection. *Journal of Artificial Intelligence Research*, 46:235–262, 2013. [1](#)
- [22] B. Han, Q. Yao, X. Yu, G. Niu, M. Xu, W. Hu, I. W. Tsang, and M. Sugiyama. Co-teaching: robust training of deep neural networks with extremely noisy labels. In *Proceedings of the 32nd International Conference on Neural Information Processing Systems*, pages 8536–8546, 2018. [3](#)
- [23] D. Hendrycks, M. Mazeika, and T. Dietterich. Deep anomaly detection with outlier exposure. *arXiv preprint arXiv:1812.04606*, 2018. [1](#), [2](#), [3](#), [14](#)
- [24] J. P. Hwang, S. Park, and E. Kim. A new weighted approach to imbalanced data classification problem via support vector machine with quadratic cost function. *Expert Systems with Applications*, 38(7):8580–8585, 2011. [1](#), [2](#)
- [25] A. Krizhevsky, G. Hinton, et al. Learning multiple layers of features from tiny images. 2009. [2](#), [6](#)
- [26] L. J. Latecki, A. Lazarevic, and D. Pokrajac. Outlier detection with kernel density functions. In *International Workshop on Machine Learning and Data Mining in Pattern Recognition*, pages 61–75. Springer, 2007. [2](#)
- [27] S. S. Lee. Noisy replication in skewed binary classification. *Computational statistics & data analysis*, 34(2):165–191, 2000. [1](#), [2](#)
- [28] C.-L. Li, K. Sohn, J. Yoon, and T. Pfister. Cutpaste: Self-supervised learning for anomaly detection and localization. *arXiv preprint arXiv:2104.04015*, 2021. [1](#), [2](#), [3](#), [4](#), [7](#), [8](#), [16](#)
- [29] J. Li, R. Socher, and S. C. Hoi. Dividemix: Learning with noisy labels as semi-supervised learning. In *International Conference on Learning Representations*, 2019. [3](#)
- [30] A. Liu, J. Ghosh, and C. E. Martin. Generative oversampling for mining imbalanced datasets. In *DMIN*, pages 66–72, 2007. [1](#), [2](#)
- [31] F. T. Liu, K. M. Ting, and Z.-H. Zhou. Isolation forest. In *2008 eighth ieee international conference on data mining*, pages 413–422. IEEE, 2008. [2](#), [3](#)
- [32] G. J. McLachlan. Iterative reclassification procedure for constructing an asymptotically optimal rule of allocation in discriminant analysis. *Journal of the American Statistical Association*, 70(350):365–369, 1975. [3](#)
- [33] E. Min, J. Long, Q. Liu, J. Cui, Z. Cai, and J. Ma. Su-ids: A semi-supervised and unsupervised framework for network intrusion detection. In *International Conference on Cloud Computing and Security*, pages 322–334. Springer, 2018. [3](#)
- [34] J. Muñoz-Marí, F. Bovolo, L. Gómez-Chova, L. Bruzzone, and G. Camp-Valls. Semisupervised one-class support vector machines for classification of remote sensing data. *IEEE transactions on geoscience and remote sensing*, 48(8):3188–3197, 2010. [3](#)
- [35] D. A. Reynolds. Gaussian mixture models. *Encyclopedia of biometrics*, 741:659–663, 2009. [2](#)
- [36] L. Ruff, R. Vandermeulen, N. Goernitz, L. Deecke, S. A. Siddiqui, A. Binder, E. Müller, and M. Kloft. Deep one-class classification. In *International conference on machine learning*, pages 4393–4402. PMLR, 2018. [1](#), [2](#), [3](#), [4](#)

- [37] L. Ruff, R. A. Vandermeulen, N. Görnitz, A. Binder, E. Müller, K.-R. Müller, and M. Kloft. Deep semi-supervised anomaly detection. In *International Conference on Learning Representations*, 2020. 1, 3
- [38] B. Schölkopf, R. C. Williamson, A. J. Smola, J. Shawe-Taylor, J. C. Platt, et al. Support vector method for novelty detection. In *NIPS*, volume 12, pages 582–588. Citeseer, 1999. 1, 2
- [39] H. Scudder. Probability of error of some adaptive pattern-recognition machines. *IEEE Transactions on Information Theory*, 11(3):363–371, 1965. 3
- [40] K. Sohn, D. Berthelot, N. Carlini, Z. Zhang, H. Zhang, C. A. Raffel, E. D. Cubuk, A. Kurakin, and C.-L. Li. Fixmatch: Simplifying semi-supervised learning with consistency and confidence. *Advances in Neural Information Processing Systems*, 33, 2020. 3
- [41] K. Sohn, C.-L. Li, J. Yoon, M. Jin, and T. Pfister. Learning and evaluating representations for deep one-class classification. *arXiv preprint arXiv:2011.02578*, 2020. 1, 2, 3, 4, 6, 7, 8, 13, 14, 15, 17
- [42] H. Song, Z. Jiang, A. Men, and B. Yang. A hybrid semi-supervised anomaly detection model for high-dimensional data. *Computational intelligence and neuroscience*, 2017. 3
- [43] D. M. Tax and R. P. Duin. Support vector data description. *Machine learning*, 54(1):45–66, 2004. 1, 2
- [44] H. Xiao, K. Rasul, and R. Vollgraf. Fashion-mnist: a novel image dataset for benchmarking machine learning algorithms. *arXiv preprint arXiv:1708.07747*, 2017. 6
- [45] Q. Xie, M.-T. Luong, E. Hovy, and Q. V. Le. Self-training with noisy student improves imagenet classification. In *Proceedings of the IEEE/CVF Conference on Computer Vision and Pattern Recognition*, pages 10687–10698, 2020. 2, 3
- [46] B. Zhang and W. Zuo. Learning from positive and unlabeled examples: A survey. In *2008 International Symposiums on Information Processing*, pages 650–654. IEEE, 2008. 1
- [47] C. Zhou and R. C. Paffenroth. Anomaly detection with robust deep autoencoders. In *Proceedings of the 23rd ACM SIGKDD international conference on knowledge discovery and data mining*, pages 665–674, 2017. 3
- [48] B. Zong, Q. Song, M. R. Min, W. Cheng, C. Lumezanu, D. Cho, and H. Chen. Deep autoencoding gaussian mixture model for unsupervised anomaly detection. In *International Conference on Learning Representations*, 2018. 1, 2, 3, 5, 6

## A Appendix

### A.1 Additional results with different metrics

There are various performance metrics of one-class classifiers. In the main manuscript, we mainly use AUC, Average Precision (AP) and F1-score as the evaluation metrics. In this subsection, we report the performances of the proposed model (STOC) and baselines in terms on Recall at Precision 70 and 90 as the additional metrics on CIFAR-10 dataset.

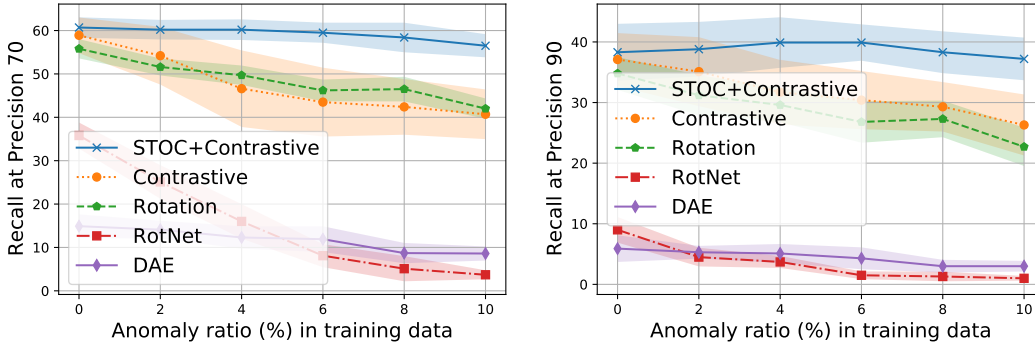


Figure 9: Performance of various one-class classifiers on CIFAR-10 dataset. STOC is applied on top of Contrastive [41]. (Left) Recall at Precision 70, (Right) Recall at Precision 90.

As in Fig. 9, we observe a similar trends with these two additional metrics as well. For example, the performances of STOC are robust across various anomaly ratios. On the other hand, all the other one-class classifiers show consistent and significant performance degradation as the anomaly ratio increases. STOC performs 15.8 and 10.9 better than the state-of-the-art one-class classifier [41] in terms of recall at precision 70 and 90, respectively.

### A.2 STOC on raw tabular features / learned image representations

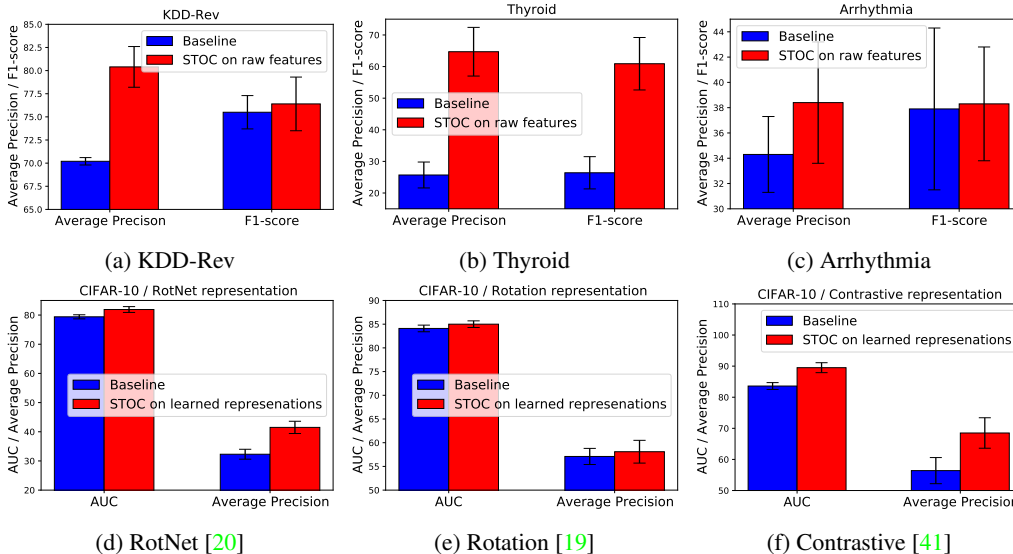


Figure 10: Performance of STOC on (top) raw tabular features and (lower) learned image representations. STOC consistently outperforms baseline and in some cases (e.g., Thyroid, and Contrastive [41]), the performance improvements are significant.

STOC is also applicable on raw tabular features or learned image representation without representation update using data refinement. In this section, we demonstrate the performance improvements by

STOC without representation update to verify the effectiveness of data refinement block of STOC for shallow one-class classifiers.

Fig. 10 (upper) demonstrates consistent and significant performance improvements when we apply STOC on top of raw tabular features. Specifically, the Average Precision (AP) improvements are 10.2, 29.0, and 4.1 with KDD-Rev, Thyroid, and Arrhythmia tabular datasets, respectively.

We also apply STOC on top of various learned image representations. As can be seen in Fig. 10 (lower), the performance improvements of STOC are consistent across various different learned image representations (without representation update). For instance, the AP improvements are 9.2, 1.0, and 12.1 with learned image representations using RotNet [20], Rotation [19], and Contrastive [41], respectively.

### A.3 Implementation Details on GOAD [5] for Tabular Data Experiments

A classification-based anomaly detection method, GOAD [5], has demonstrated strong anomaly detection performance on tabular datasets. Unlike previous works [20, 23] that formulate a parametric classifier for multiple transformation classification, GOAD employs distance-based classification of multiple transformations. For the set of transformations  $T_m : \mathcal{X} \rightarrow \mathcal{D}$ ,  $m = 1, \dots, M$ , the loss function of GOAD is written as in Equation (3) with the probability defined in Eq. (4).

$$\mathcal{L} = -\mathbb{E}_{m,x} [\log P(m|T_m(x))], \quad (3)$$

$$P(\hat{m}|T_m(x)) = \frac{\exp(-\|f(T_m(x)) - c_{\hat{m}}\|^2)}{\sum_n \exp(-\|f(T_m(x)) - c_n\|^2)}, \quad (4)$$

where the centers  $c_m$ 's are updated by the average feature over the training set. While it is shown to perform well [5], we find that the distance-based formulation is not necessary, and we achieve the similar performance, if not worse, to [5] using a parametric classifier when computing the probability:

$$P(\hat{m}|T_m(x)) = \frac{\exp(w_{\hat{m}}^\top f(T_m(x)) + b_{\hat{m}})}{\sum_n \exp(w_n^\top f(T_m(x)) + b_n)} \quad (5)$$

The formulation in Eq. (5) is easier to optimize than its original form in Eq. (4) as it can be fully optimized with backpropagation without alternating updates of feature extractor  $f$  and centers  $c_m$ . Once we learn a representation by optimizing the loss in Equation (3) using Equation (5), we follow a two-stage one-class classification framework of [41] to construct a set of Gaussian density estimation one-class classifiers for each transformation. Finally, we aggregate a maximum normality scores from a set of classifiers as the normality score.

In Table 1, we summarize the implementation details, such as network architecture or hyperparameters, and anomaly detection performance under N setting that reproduces the results in [5].

Datasets	KDD	KDD-Rev	Thyroid	Arrhythmia
F-score [5]	98.4±0.2	98.9±0.3	74.5±1.1	52.0±2.3
F-score (ours)	98.0±0.2	95.0±0.2	75.1±2.4	54.8±3.2
$f$ (feature)	[Linear(8), LeakyReLU(0.2)] × 5			
Optimizer	Momentum SGD (momentum=0.9)			
Learning rate	0.001			
L2 weight regularization	0.00003			
Batch size	64 × $M$			
Random projection dimension	32			
$M$ (number of transformations)	32		256	
Train steps	$2^{10}$		$2^{16}$	

Table 1: The anomaly detection performance under N setting of GOAD in [5] and our implementation. Our implementation demonstrates comparable, if not worse, performance to those reported in [5]. Our implementation also shares most hyperparameters across datasets except the  $M$ , the number of transformations, and the train steps, which are closely related to the size of training data.

#### A.4 Per-class AUC and AP

In the main manuscript, we report the mean and standard deviation of AUC and AP across all classes in each dataset. In this section, we report the mean and standard deviation of AUC and AP for each class in each dataset (including CIFAR-10 (Table 2), MVTec AD (Table 3), fMNIST (Table 4), and Dog-vs-Cat (Table 5) datasets).

##### A.4.1 Per-class AUC and AP on CIFAR-10 dataset

anomaly ratios	0%		10%	
Classes / Methods	Baseline [41]	STOC + [41]	Baseline [41]	STOC + [41]
AUC				
Airplane	90.5±0.6	90.4±0.4	85.3±0.8	87.6±0.7
Automobile	98.8±0.1	98.7±0.1	95.2±0.5	97.9±0.3
Bird	87.5±0.6	87.1±0.8	75.6±1.1	84.7±1.2
Cat	81.5±0.5	80.3±0.7	68.9±1.0	78.5±1.5
Deer	90.3±0.4	90.2±0.5	79.9±0.8	87.4±0.5
Dog	90.8±0.7	90.8±0.6	79.2±2.5	89.6±0.6
Frog	92.0±0.6	91.4±0.9	78.5±2.1	87.5±1.3
Horse	97.8±0.1	97.9±0.1	93.3±0.5	96.0±0.6
Ship	96.5±0.2	96.4±0.1	91.5±0.9	95.2±0.5
Truck	95.1±0.3	95.8±0.1	88.9±0.4	94.7±0.4
Average Precision				
Airplane	68.3±1.7	67.9±1.1	61.3±1.9	61.8±1.1
Automobile	93.9±0.2	94.1±0.1	85.9±3.4	91.5±0.7
Bird	62.2±2.1	61.7±2.4	42.4±3.0	57.5±2.3
Cat	44.0±2.4	42.9±1.9	30.3±3.8	44.9±0.9
Deer	59.5±0.8	58.8±1.2	42.9±3.5	53.6±1.5
Dog	59.1±6.5	59.8±4.7	39.7±9.1	64.5±2.0
Frog	72.7±2.0	70.4±6.9	38.5±11.0	73.6±3.6
Horse	89.0±0.7	89.2±0.6	80.6±1.9	86.2±1.1
Ship	83.9±0.8	83.7±0.6	74.9±2.4	79.8±0.7
Truck	79.0±1.6	81.3±0.4	67.0±1.9	75.8±1.2

Table 2: The anomaly detection performance per class on CIFAR-10 dataset in terms of AUC and AP. Class represents the label of normal samples.

#### A.4.2 Per-class AUC and AP on MVTec AD dataset

anomaly ratios	0%		10%	
Classes / Methods	Baseline [28]	STOC + [28]	Baseline [28]	STOC + [28]
AUC				
Bottle	98.0±1.0	98.8±0.7	94.3±0.8	98.7±0.7
Cable	77.7±0.7	77.9±2.6	72.9±3.3	80.4±0.9
Capsule	96.1±1.1	97.2±1.3	92.4±1.7	96.8±0.7
Hazelnut	97.2±0.7	97.5±0.4	83.5±3.6	96.7±0.6
Metal Nut	98.5±1.0	98.6±0.4	91.2±2.8	98.7±0.3
Pill	92.1±3.1	91.1±2.5	85.1±1.5	92.1±0.5
Screw	87.4±1.6	86.8±2.5	79.9±1.0	86.4±1.4
Toothbrush	98.5±1.5	98.3±1.1	98.6±1.3	99.3±1.2
Transistor	96.4±2.0	96.7±1.6	93.9±2.8	95.7±0.7
Zipper	99.4±0.4	98.0±0.6	91.1±2.9	99.2±0.7
Carpet	90.0±3.9	90.8±4.6	80.4±6.1	91.2±2.7
Grid	99.2±0.5	99.7±0.3	92.9±7.6	99.7±0.2
Leather	99.8±0.3	99.7±0.4	98.0±1.1	100.0±0.0
Tile	93.1±1.5	93.3±2.7	86.4±3.4	92.4±1.8
Wood	98.8±0.9	98.5±1.4	92.1±2.2	99.0±0.5
Average Precision				
Bottle	98.8±0.7	99.3±0.5	94.3±1.6	98.0±0.6
Cable	81.8±0.9	82.3±1.7	70.8±4.3	74.1±3.0
Capsule	99.0±0.3	99.3±0.3	79.5±5.3	89.8±2.7
Hazelnut	97.1±0.6	97.0±0.4	88.8±3.6	93.6±1.9
Metal Nut	99.6±0.3	99.6±0.1	76.1±8.4	92.1±3.1
Pill	98.2±0.7	97.9±0.6	56.6±2.6	67.3±2.2
Screw	93.8±1.1	93.6±1.3	60.1±2.8	63.7±1.8
Toothbrush	99.2±0.9	99.2±0.6	97.4±2.2	98.6±2.0
Transistor	93.0±3.0	93.7±2.4	97.8±1.6	97.1±0.5
Zipper	99.8±0.2	99.2±0.3	86.1±2.8	98.0±1.5
Carpet	94.4±3.5	95.7±2.8	64.2±8.2	71.6±4.2
Grid	99.5±0.3	99.8±0.2	90.9±6.1	99.4±0.4
Leather	99.9±0.2	99.9±0.2	97.2±1.3	100.0±0.1
Tile	96.1±0.9	96.4±1.4	82.4±4.5	86.4±2.8
Wood	99.4±0.5	99.4±0.6	88.1±3.2	97.2±1.7

Table 3: The anomaly detection performance per class on MVTec AD dataset in terms of AUC and AP. Class represents the label of normal samples.



### A.4.3 Per-class AUC and AP on fMNIST dataset

anomaly ratios	0%		10%	
Classes / Methods	Baseline [41]	STOC + [41]	Baseline [41]	STOC + [41]
AUC				
T-shirt/top	93.3±1.2	93.2±1.0	79.2±1.3	84.7±1.0
Trouser	99.2±0.3	99.2±0.2	92.9±0.8	94.5±1.9
Pullover	93.8±0.2	93.8±0.2	78.4±2.7	90.1±1.1
Dress	94.4±0.5	94.0±0.5	78.4±3.5	85.8±1.6
Coat	95.1±0.1	94.9±0.2	80.4±3.1	88.7±1.7
Sandal	95.4±0.3	95.5±0.4	67.6±4.3	81.7±1.8
Shirt	87.9±0.2	87.9±0.2	73.9±1.2	81.0±2.5
Sneaker	99.1±0.0	99.2±0.1	80.2±4.9	94.7±3.6
Bag	97.8±0.2	97.6±0.3	58.2±3.3	68.6±2.3
Ankle boot	98.6±0.2	98.5±0.2	76.6±2.6	87.1±3.6
Average Precision				
T-shirt/top	68.7±12.1	67.9±8.9	43.0±4.7	56.8±3.7
Trouser	96.5±2.9	98.2±0.3	78.2±5.2	87.1±3.7
Pullover	62.7±1.2	63.6±1.3	27.2±6.9	57.1±1.5
Dress	72.3±3.7	71.6±2.7	36.1±8.8	57.3±2.6
Coat	66.2±1.1	65.6±1.0	24.3±3.9	50.7±9.5
Sandal	70.9±2.8	70.8±2.4	17.8±5.9	40.1±5.4
Shirt	49.6±0.9	49.7±0.9	27.2±5.8	37.6±4.7
Sneaker	91.9±0.4	92.9±0.9	21.0±3.8	81.6±11.4
Bag	92.2±0.4	91.8±1.0	13.2±2.0	20.1±3.7
Ankle boot	87.9±1.4	86.5±1.5	19.6±3.1	48.0±16.5

Table 4: The anomaly detection performance per class on fMNIST dataset in terms of AUC and AP. Class represents the label of normal samples.

### A.4.4 Per-class AUC and AP on Dog-vs-Cat dataset

anomaly ratios	0%		10%	
Classes / Methods	Baseline [41]	STOC + [41]	Baseline [41]	STOC + [41]
AUC				
Dog	89.7±0.6	89.2±0.4	74.7±2.1	79.1±1.3
Cat	88.2±0.4	88.0±0.7	70.1±2.4	70.7±1.8
Average Precision				
Dog	91.6±0.7	91.0±0.6	80.0±2.2	84.0±1.2
Cat	90.2±0.3	89.8±1.0	71.6±3.8	71.5±4.8

Table 5: The anomaly detection performance per class on Dog-vs-Cat dataset in terms of AUC and AP. Class represents the label of normal samples.